CISTER
Research Centre in
Real-Time & Embedded
Computing Systems

Conference Paper

Wireless radio link design to improve near-shore communication with surface nodes on tidal waters

Miguel Gutiérrez Gaitán*
Pedro d'Orey*
Pedro Miguel Santos*
Manuel Ribeiro
Luis Pinto
Luís Almeida*
J. Borges de Sousa

*CISTER Research Centre

CISTER-TR-210706

2021/09/20

Wireless radio link design to improve near-shore communication with surface nodes on tidal waters

Miguel Gutiérrez Gaitán*, Pedro d'Orey*, Pedro Miguel Santos*, Manuel Ribeiro, Luis Pinto, Luís Almeida*, J. Borges de Sousa

*CISTER Research Centre

Rua Dr. António Bernardino de Almeida, 431

4200-072 Porto

Portugal

Tel.: +351.22.8340509, Fax: +351.22.8321159

E-mail: mjggt@isep.ipp.pt, ore@isep.ipp.pt, pss@isep.ipp.pt, maribeiro@fe.up.pt, pin@isep.ipp.pt, lda@fe.up.pt, jtasso@fe.up.pt

https://www.cister-labs.pt

Abstract

Wireless radio links deployed over aquatic areas (e.g., sea, estuaries or harbors) are affected by the conductive properties of the water surface, strengthening signal reflections and increasing interference effects. Recurrent natural phenomena such as tides or waves cause shifts in the water level that, in turn, change the interference patterns and cause varying impairments to propagation over water surfaces. In this work, we aim at mitigating the detrimental impact of tides on the quality of a line-of-sight over-water link between an onshore station and a surface node, targeting mission data transfer scenarios. We consider different types of surface nodes, namely, autonomous underwater vehicles, unmanned surface vehicles and buoys, and we use WiFi technology in both 2.4 GHz and 5 GHz frequency bands. We propose two methods for link distance/height design: (i) identifying a proper Tx-Rx distance for improved link quality at each point of the tidal cycle; (ii) defining the height/distance that minimizes the path loss averaged during the whole tidal cycle.Experimental results clearly show the validity of our link quality model and the interest of method (i). Analytical results confirm method (ii) and show that it outperforms, in both frequency bands, the common practice of placing onshore antennas at the largest possible height and/or surface nodes at a short but arbitrary distance.

Wireless radio link design to improve near-shore communication with surface nodes on tidal waters

Miguel Gutiérrez Gaitán*†‡, Pedro M. d'Orey‡, Pedro M. Santos†, Manuel Ribeiro¶, Luís Pinto§, Luís Almeida‡, and J. Borges de Sousa¶

***Abstract*—Wireless radio links deployed over aquatic areas (e.g., sea, estuaries or harbors) are affected by the conductive properties of the water surface, strengthening signal reflections and increasing interference effects. Recurrent natural phenomena such as tides or waves cause shifts in the water level that, in turn, change the interference patterns and cause varying impairments to propagation over water surfaces. In this work, we aim at mitigating the detrimental impact of tides on the quality of a line-of-sight over-water link between an onshore station and a surface node, targeting mission data transfer scenarios. We consider different types of surface nodes, namely, autonomous underwater vehicles, unmanned surface vehicles and buoys, and we use WiFi technology in both 2.4 GHz and 5 GHz frequency bands. We propose two methods for link distance/height design: (i) identifying a proper Tx-Rx distance for improved link quality at each point of the tidal cycle; (ii) defining the height/distance that minimizes the path loss averaged during the whole tidal cycle. Experimental results clearly show the validity of our link quality model and the interest of method (i). Analytical results confirm method (ii) and show that it outperforms, in both frequency bands, the common practice of placing onshore antennas at the largest possible height and/or surface nodes at a short but arbitrary distance.**

***Index Terms*—maritime communication, over-water, path loss, propagation, tidal fading, tides, two-ray, wireless, WiFi.**

I. Introduction

Wireless radio data links are nowadays a common infrastructure support for remote maritime operations [1]. Modern monitoring and/or control systems operating in aquatic environments (e.g. offshore aquaculture [2], surveillance [3], oceanographic research [4]) are gradually adopting radio-frequency (RF) communication technology for data transfer. Yet, achieving adequate RF communication performance in water environments is still challenging because of the multiplicity of factors impacting the quality of the over-water channel [5]. The conductive properties of the water medium and the relatively flat surface make radio signal reflections stronger, potentially causing a severe interference phenomenon known as deep fading [6], [7]. Natural water movements, such as tides and waves, further impair RF signal propagation superimposing additional fading effects [7]–[10].

The influence of tides on the link quality is particularly noticeable near shore and whenever the relative height to the water surface of (one of) the nodes varies. Destructive interference causes the so-called *nulls* that could move over time according to the tide [11]. Similarly, *tidal fading* [12], i.e., the recurrent impact of tides on the mean path loss experienced in a link, has been shown to be tremendously detrimental at specific combinations of link distance and antenna height [13]. These two phenomena are predicted by the well-known two-ray propagation model [6]. Conventional methods to counteract tidal related issues often rely on classical diversity techniques, e.g., space-diversity [14] or frequency-diversity [13], thus generally requiring additional communication resources (e.g., a second receiver hardware), which may not always be available or feasible. To address such limitation, a technique was recently proposed in [15], which leverages the basis of the two-ray model to find an optimal antenna height design that mitigates average path loss for shore-to-shore links operating over tidal waters.

However, research on this topic is generally scarce and mostly focused on the long-range case, typically considering links of kilometric distances [12]–[14], thus not being directly applicable to the near-shore case. Moreover, the impact of tidal fading on Line-of-Sight (LOS) shore-to-surface links is often ignored, despite being a quite common issue in practice, for both moving and stationary nodes. For example, Autonomous Underwater Vehicles (AUVs) come to the surface momentarily to offload data to an onshore gateway and update mission information [16]. Likewise, Unmanned Surface Vehicles (USVs) [17] can gather data from a surrounding area and offload it to an onshore gateway at a desired moment. In other cases, we may have mooring nodes such as floating sensors [18] or buoys for coastal monitoring [19] possibly doing regular data transmission [10] over long periods w.r.t. the tidal cycle.

In this work, we target the case of over-water RF links between onshore stations and both stationary or moving surface nodes (e.g. buoys, USVs and AUVs) operating at near-shore, within a few tens to few hundreds of meters. We assume that these links are deployed over tidal waters, which effectively change the relative antenna-to-surface height at the onshore station side, only. We consider the two situations referred above, namely **mobile nodes** (e.g., USVs or AUVs) that communicate data occasionally but intensively for a relatively short period of time (few seconds to few minutes), and **stationary nodes** (e.g., buoys or floating mooring nodes) that recurrently transmit data either continuously or for extended periods of time (hours to months or even years).

For each situation we provide a method that allows improv-

*Facultad de Ingeniería, Universidad Andres Bello, Santiago, Chile
†FEUP, Universidade do Porto, Portugal – {mgg, lda}@fe.up.pt
‡CISTER Research Center, Porto, Portugal – {mjggt, ore, pss}@isep.ipp.pt
§IPFN, Instituto Superior Técnico, Portugal – lpinto@ipfn.tecnico.ulisboa.pt
¶LSTS, Universidade do Porto, Portugal – {maribeiro,jtasso}@fe.up.pt

ing the link quality by determining the antenna height and/or node positioning dynamically or in the design phase. Both methods rely on the commonly used two-ray model. Method (i) considers the tide level, possibly inferred from an accurate tidal model, in combination with the two-ray model to compute the distance at which the maximum signal strength occurs after the last null. Mobile surface vehicles can then be instructed to move to such region and then initiate communication with the station on shore. Method (ii) allows optimizing the positioning of the surface nodes and/or the height of the onshore antenna to minimize average path loss over the full tidal cycle, thus providing an improved communication link on average.

An experimental campaign in a harbor with a floating AUV using WiFi technology in the 2.4 GHz band for data transfer to an on shore node validated simultaneously the applicability of the two-ray model to this technology as well as method (i). Then, we provide analytical results of method (ii) to determine the distance/height design regions of least average path loss scenario for stationary surface nodes. We carry out this analysis for two frequency bands, namely 2.4 GHz and 5 GHz, concluding that method (ii) is dominant, in both bands, against the common practice of placing onshore antennas as high as feasible and/or floating nodes at a short but arbitrary distance from the shore.

The remainder of this paper is organized as follows. Section II provides the theoretical basis of the two-ray model and revisits its expression in the presence of tides. Section III introduces the problem considering both the determination of the region of nulls as well as the antenna height on shore and the position of the stationary surface nodes that minimize average path loss. Section IV reports the results from a shore-AUV experimental campaign as well as the analytical results for path loss minimization. Section V reviews the relevant literature and highlights the main contributions of this work. Finally, Section VI concludes the paper.

II. The Two-Ray Propagation Model

This section presents the RF signal propagation model in the presence of tides, and motivates the study from the perspective of the shore-to-surface overwater channel at near-shore.

A. The two-ray model

The two-ray propagation model is a fundamental method to account for the impact of surface reflections on wireless radio links [6]. It describes, essentially, the Received Signal Strength (RSS) of the link as the vectorial summation of two copies of the same transmitted signal that reach the receiver following two different trajectories: (1) a direct line-of-sight (LoS) path from the transmitter to the receiver, and (2) an indirect path, reflected from the surface. The length of these two paths is different, and thus, there is a phase shift between the two copies of the signal when arriving at the receiver side. This, in turn, leads to a self-interference pattern on the RSS, which can be severely destructive (or either constructive), depending - among other parameters - on the resulting geometry of the link.

Formally, the two-ray model can be expressed as the average power received on the link P_r (in W) as function of the link distance (d) and the respective antenna heights of the transmitter (h_t) and the receiver (h_r), as show in Eq. 1.

$$P_r = \frac{\lambda^2}{(4\pi d)^2}\left[2\sin\left(\frac{2\pi h_t\, h_r}{\lambda d}\right)\right]^2 P_t G_t G_r \qquad (1)$$

where $\lambda = c/f$ is the wavelength (with c the speed of light and f the operating frequency), P_t the transmitted power, and G_t and G_r the respective transmitter and receiver antenna gains.

B. The two-ray model over tidal waters

From the perspective of the two-ray propagation model, a rise and fall of the water level due to tides will recurrently modify the geometry of the link [11]. Then, for the case of shore-to-surface links, this effect will only change the relative antenna-to-surface height of onshore nodes. This effect does not occur on surface nodes (e.g. buoys, USVs), since when these are floating, this implies that their antenna heights are always constant w.r.t. the water surface.

Based on these observations, we revisit the two-ray model expression in Eq. 1, by incorporating a small water-level variation Δ_k, which solely influences the relative antenna-to-surface height of the onshore node, as illustrated in Fig. 1. We denote Tx as the *onshore* transceiver device, for which we assume an effective antenna height $h_t = h_0 + \Delta_k$, being h_0, a nominal antenna height w.r.t. a long-term average water level. Then, we denote the receiving transceiver by Rx, and h_r as its corresponding antenna height, which as stated before, remains always constant regardless of the (slow) water level dynamics[1].

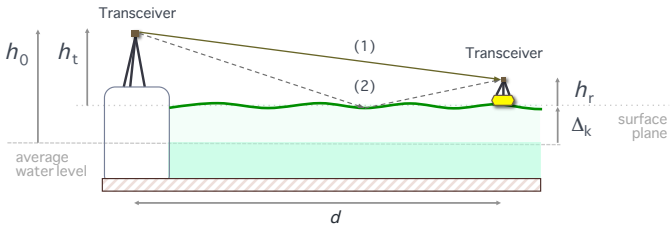

Fig. 1: The two-ray model showing: (1) the direct LoS ray, and (2) the indirect ray reflected from the surface when experiencing a water level variation of Δ_k.

Formally, the modified expression for the two-ray model applied to the case of a shore-to-surface link deployed over tidal waters is presented as follows:

$$P_r = \frac{\lambda^2}{(4\pi d)^2}\left[2\sin\left(\frac{2\pi(\boldsymbol{h_0 + \Delta_k})\, h_r}{\lambda d}\right)\right]^2 P_t G_t G_r \qquad (2)$$

[1]We consider the transmitter on shore and the receiver on the surface node just as an example. The two-ray model is symmetrical and the roles of the nodes can be switched without any impact on the analysis.

Eq. 2 can be alternately represented in terms of the average path losses (in dB) experienced by the link, as shown in Eq. 3.

$$L_{2ray} = -10\log_{10}\left(\frac{\lambda^2}{(4\pi d)^2}\left[2\sin\left(\frac{2\pi(h_0+\Delta_k)h_r}{\lambda d}\right)\right]^2\right) \quad (3)$$

We further note that this expression is independent of the transmission power and the T_x and R_x antenna gains, which do not influence the path loss behaviour. Although trivial, we present this expression extension here for completeness, since it is relevant for the understanding of the path loss optimization method proposed in Section IV.

Illustrative example. To better understand how the two-ray model behaves in the near-shore region in a concrete case, we plot the received signal strength variation in Fig. 2, corresponding to Eq. 1 expressed in dBm. In this case, the surface node antenna height is short (few cms), that of an AUV on the surface, and the antenna on shore is on a quay in a harbor. For very short distances we see sudden changes from destructive to constructive interference until a point at which we observe the deepest and last destructive interference area. After this last null the signal strength increases significantly and then decreases smoothly as the T_x-R_x separation increases. The figure shows the signal strength as a function of the distance to the shore for two close but different moments in the tide (30 cm difference in height). Interestingly, as the height increases (lower tide), the last null shifts to a higher distance, moving together the area of destructive interference (high loss).

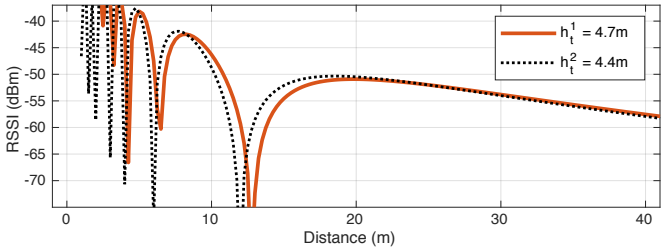

Fig. 2: Received Signal Strength (RSS) as a function of the distance to shore in the near-shore region, for two moments in the tide, leading to two slightly different antenna heights.

To complement this brief study on the impact of variations of antenna height in the model outcome, we looked into the same case of an AUV operating as a surface vehicle but applied small variations to its already short antenna height. We used the same setting as above with an onshore antenna at 4.7 m above the water level and the AUV antenna at 17 ± 2 cm. The results shown in Fig. 3 reveal that such differences, even if small, cause a further shift of more than $\pm$1m in the position of the last null. Particularly, at 19 cm height, the null gets closer to $d = 15m$.

III. Problem Formulation

As stated previously, we consider two cases, namely for dynamic and stationary surface nodes. For each of these situations we formulate the following optimization problems.

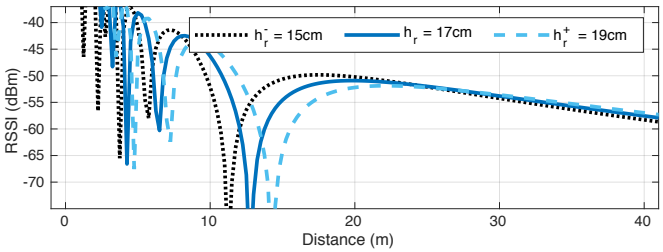

Fig. 3: Received Signal Strength (RSS) as a function of the distance to shore in the near-shore region, for small deviations in the antenna height for low antennas on the surface node.

A. Link distance design for dynamic surface nodes

Consider a mobile surface node, either an USV or an AUV at the surface, that executes a mission in a given area and, at some point in time, needs to communicate intensively, in a short time interval, with a base station on shore, be it for data offloading or for acquiring new mission information.

The problem consists on determining a convenient distance to shore d_{conv} that will lead to sustained high received signal strength in a broad region so that the vehicle can be driven to that distance and initiate communication reliably. For example, in the situation of Fig. 2, $d_{conv} \approx 20$ m would be adequate. A suitable value can be determined numerically as the local maximum after the last null, as in Eq. 4.

$$d_{conv} = max(d) : \frac{\partial P_r(d)}{\partial d} = 0 \quad (4)$$

A good region for communication would be between d_{conv} and $2 * d_{conv}$, which is further way from the last null and exhibits just about 7 dBm attenuation with respect to the maximum at d_{conv}. However, in order to solve Eq. 4 it is necessary to define the height of the antennas. On the vehicle side, the antenna height is fixed and known. However, on shore the antenna height depends on the tide. Therefore, solving this problem requires knowing the tide, e.g. with an accurate tidal model, or by direct measurement (e.g. using an acoustic sensor)[2]. Then, the vehicle can position itself in a convenient region for improved communication.

B. Ant. height/link distance design for stationary surface nodes

Consider now a stationary surface node (e.g., a buoy or floating mooring node) that communicates regularly with a station on shore (e.g. a gateway or base station), either continuously or over a long period w.r.t. the tidal cycle, i.e the communication link is affected by tidal fading. To mitigate this effect we propose a method for defining the antenna height or link distance that minimizes average communication path loss over a full tidal cycle, providing the best average channel conditions.

[2]Note that, for a particular vehicle with fixed and known antenna height, it is possible to tabulate the value of d_{conv} for a range of heights of the onshore antenna corresponding to the different moments in the tidal cycle.

To solve this problem we build on the method in [15] originally proposed to provide an optimal antenna-height design for shore-to-shore links over tidal waters. We adapt it herein for the case of shore-to-surface links for determining an optimal antenna height for the onshore node when communicating with a surface node over the duration of a tidal cycle. Along the same line, we further extend the method to find the most convenient surface node position when the antenna height of the onshore node is given.

1) Antenna-height optimization: The problem of finding the nominal antenna height of the transmitter h_0 that minimizes the average path losses experienced over a finite number of Δ_k values of a given tidal range can be adapted from [15] and formally expressed as:

$$\begin{aligned} \underset{\boldsymbol{h_0}}{\text{minimize}} \quad & \frac{1}{N}\sum_{k=1}^{N} L_{2ray}(d, h_0, \Delta_k) \\ \text{subject to} \quad & \Delta_k \in [\Delta_L \ \Delta_H], \ \forall k \in [1 \ N], \\ & h_0 \in [h_0^{min} \ h_0^{max}] \end{aligned}$$

where $N \in \mathbb{N}$ is the number of steps of the discretized tidal range where the optimization expression is evaluated; Δ_k is the water level variation at the k^{th} step within the tidal range $[\Delta_L \ \Delta_H]$; and $[h_0^{min} \ h_0^{max}]$ is the h_0 feasibility region.

2) Surface node positioning: The problem of finding the most convenient positioning d for the surface-node is equivalent to the method presented in Section III-B1, i.e., targeting to find an output that minimizes average path losses over a finite number of Δ_k values of a given tidal range $[\Delta_L \ \Delta_H]$. The main difference lies in the fact that now h_0 is given, and the output d is constrained to a distance feasibility range $[d_{min} \ d_{max}]$. Formally, the problem can be expressed as follows

$$\begin{aligned} \underset{\boldsymbol{d}}{\text{minimize}} \quad & \frac{1}{N}\sum_{k=1}^{N} L_{2ray}(d, h_0, \Delta_k) \\ \text{subject to} \quad & \Delta_k \in [\Delta_L \ \Delta_H], \ \forall k \in [1 \ N], \\ & d \in [d_{min} \ d_{max}]. \end{aligned}$$

IV. Evaluation

In this section, we present two different sets of results, namely experimental results for Problem A that also validate the simple propagation model on which this work is based, and analytical results for Problem B that confirm that our approach to mitigate tidal fading on average is superior than other techniques commonly used in practice.

A. Shore-to-dynamic node WiFi link in LoS conditions

Setup. We study shore-to-AUV communication links operating in the 2.4 GHz frequency band using an existing AUV testbed. The measurement campaign was conducted in the Port of Leixões, Matosinhos, Portugal during July 2021. The shore node was placed in a concrete pier of the harbour at the following approximate location: 41.18527, -8.704882. We collected packet-based measurements of Received Signal Strength Indicator (RSSI) from a Light Autonomous Underwater Vehicle (LAUV) *Xplore-4* using the standard interface provided by the manufacturer [20]. The AUV was set to operate autonomously following a predetermined path. The AUV exchanged data (e.g telemetry data) with the *Manta* gateway (GW) through a WiFi link, which functioned as Access Point (AP) for the network. This setup allowed us to monitor and control the vehicle in case of need, which was particularly useful close to the quay (up to $\sim$30 m) where, a few times, the AUV required manual operation. Fig. 4(a) shows the testbed setup at the actual location, including the portable gateway, the AUV and the remote operator.

The AUV performed 15 equivalent round-trip missions starting from the quay and moving way from this structure until reaching up to approximately 100 m. The distances were obtained based on the AUV positions acquired using a high-precision GPS device. In all the cases, the AUV was configured to operate at a low speed ($\sim$ 1m/s) as a surface vehicle, thus it was never completely submerged when on mission. The antenna height of the AUV was kept constant at $\sim$17 cm above the water surface. The gateway antenna height was $\sim 4.4 - 4.7$ m above the water surface. The difference of $\sim$ 30 cm is due to the tide water level that changed over the experiments duration, between the first and the last AUV missions. All the heights were obtained using a conventional measuring tape, to the best of our capabilities.

Experimental results. Figure 4(b)(top) shows the aggregated RSSI measurements collected at the AUV when using the setup above described. Figure 4(b)(bottom) presents the corresponding theoretical output of the two-ray model when using Eq. 1 (in dBm) and considering the simulation parameters given in Table I. Note that most parameters were selected according to the testbed setup, except for the product of the T_x power and the antenna gains, which was arbitrarily set to $P_t \cdot G_t \cdot G_r = 10$ dBm. This value simply offsets the output of the model vertically, not affecting the shape of the function, particularly the position of its minima and maxima.

TABLE I: Two-ray model parameters.

Variable	Description	Value
h_t	T_x antenna height	4.7 m
h_r	R_x antenna height	17 cm
f	Carrier frequency	2.4 GHz
d	Link distances	[1 105] m
P_t	T_x power	10 dBm
G_t,G_r	T_x and R_x antenna gains	1 dBi

We further explored the influence of the 30 cm change in the tide level that occurred during the experiments time span. Fig. 2 shows the model output for the $[0\ 20]$m range and the two extreme values of antenna height. We can see a $\sim$ 1m shift in the null position to the right when increasing the antenna height. Fig. 5 shows the RSSI measurements obtained in the first two trips of the vehicle, in the beginning of the experiment when

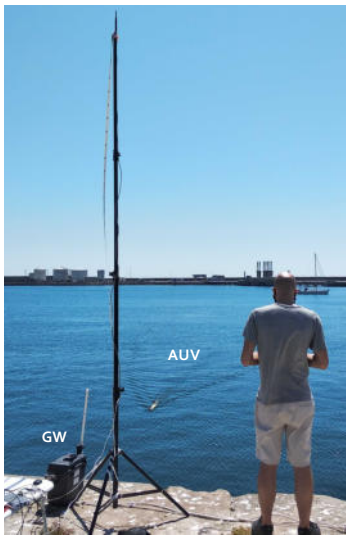

(a) Testbed setup.

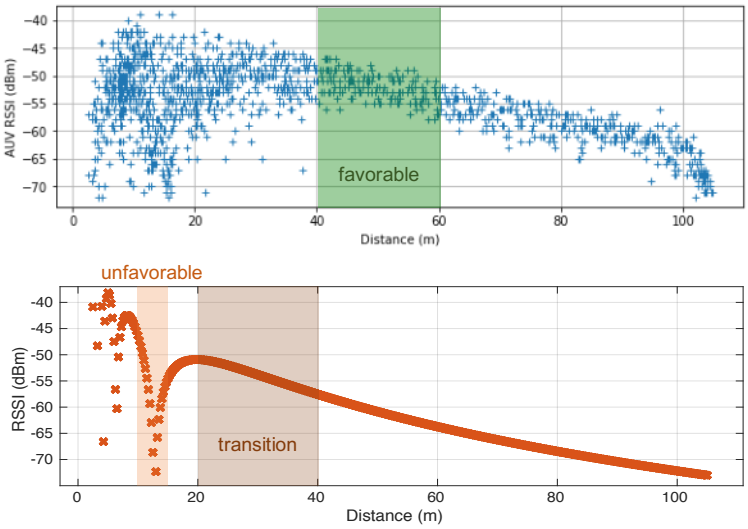

(b) RSSI measurements (top) and two-ray model (bottom).

Fig. 4: Shore-to-AUV measurements for a Wi-Fi link in line-of-sight (LOS) showing: (a) the testbed setup at the actual location, (b)(top) the RSSI measurements from the AUV over distance, and (b)(bottom) the two-ray propagation model prediction.

the antenna height was ~ 4.4m (top), and those obtained in the last two trips, at the end of the experiment when the antenna height was ~ 4.7m (bottom). A similar shift to the right is observed, despite the high variability of the RSSI signal.

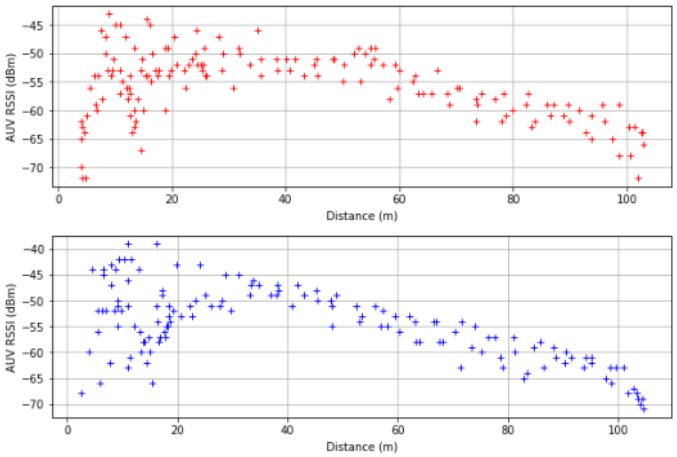

Fig. 5: RSSI measurements in the beginning of the campaign (top) and at the end of the campaign (bottom), with a tide difference of ~ 30cm.

The theoretical results obtained with the two-ray model show a good agreement in terms of the path loss dynamics experienced by the AUV measurements, particularly predicting the significant drop in the RSSI (null) at ~ 15m. The actual measurements seem to indicate a slight shift of the null to the right, from the estimated $12-13$m to closer to ~ 15m. This can be caused by a slight increase in the actual antenna height in the AUV side while it is travelling (e.g., caused by roll oscillations or due to changes in water salinity affecting the AUV floating line), as predicted in Fig. 3.

Another slight difference is the speed of decay of measured RSSI as a function of the Tx-Rx distance which is not as steep as estimated by the model. This has a direct impact in the approach suggested to solve Problem A. In fact, the actual measurements in the range between d_{conv} and $2 * d_{conv}$ still show some signal strength instability ($[20, 40]$ m in Fig. 4). Conversely, the range between $2 * d_{conv}$ and $3 * d_{conv}$ ($[40, 60]$ m) shows better stability. This area is represented by the solid green semi-circle in Fig. 6, while the area suggested by the model appears in brown.

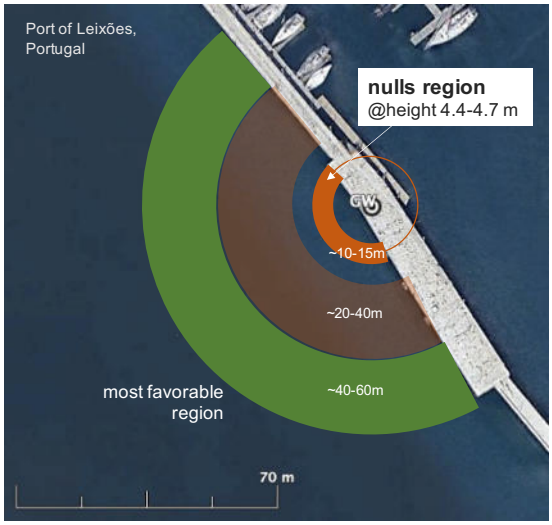

Fig. 6: Top view of the quay in the harbor showing favorable (solid green), transition (brown) and unfavorable (red) regions for the shore-to-AUV WiFi link.

Overall, we believe that the RSSI measurements show an

outstanding conformity with the theoretical prediction of the two-ray model, confirming the suitability of this model to describe the large-scale fading behavior on the shore-to-surface LOS links, even with WiFi technology and its advanced modulation techniques. A thorough revision of other relevant factors/parameters, e.g. antenna radiation pattern, cable losses, antenna directivity, diffraction, etc., can be useful to provide more accurate characterization of the channel in future work.

B. Shore-to-stationary node link in LoS conditions

Simulation setup. In order to test method (ii) for surface nodes that communicate continuously or for long periods of time (Problem B), we carry out a set of simulations that cover a wide space of configurations of interest. In particular we explore the range of link distances $d \in [10\ 1000]$ m and of heights $h_0 \in [3\ 6]$ m of the antenna onshore. We also focus on the onshore antenna height optimization since this is the most common problem, given that the surface nodes positions are frequently determined by other factors (e.g., feasibility and application criteria). We assume the use of WiFi devices operating in the 2.4 GHz and 5 GHz frequency bands and a set of receiver antenna heights $h_r = \{0.3, 0.6, 1.2\}$ m characterizing different surface nodes, from floating mooring nodes close to the water to buoys of different sizes. Finally, we consider a relatively small tidal range $[-0.5, 0.5]$ m, which we step through with a step-size $\Delta_k = 0.1$ m. Table II summarizes these parameters.

TABLE II: Simulation Setup.

Variable	Description	Value
h_t	T_x antenna height	[3,6] m
h_r	R_x antenna height	{0.3,0.6,1.2} m
f	Carrier frequency	{2.4,5.0} GHz
d	Link distances	[10, 1000] m
$[\Delta_L, \Delta_H]$	Tidal range	[-0.5, 0.5] m
Δ_k	Step-size	0.1 m

Simulation results. Fig. 7 shows the average path loss as a function of the link distance d obtained by our antenna-height design method (solid blue line) detailed in Section III-B1. For benchmarking purposes, we also plot the path loss achieved when the onshore antenna is placed at the largest feasible height (dashed yellow line), which is common practice. Finally, we contrast both approaches against the worst case scenario (dotted red line), i.e., the antenna height within the h_0 feasibility range that maximizes the average attenuation for each link distance.

As expected, given our optimal design method, our results are always better (or equal) than using the onshore antenna at the top of the feasibility range. Fixing the antenna at the top leads to strong variations in average attenuation in the near-shore region of the link, varying between the worst-case and the best-case for close link distances. A similar behavior also occurs with any fixed antenna height. This shows the importance of careful choice of a specific antenna height for each target distance, particularly in the near-shore region. The results also show that the near-shore region expands significantly with the antenna height of the surface node, from 0.3m to 1.2m, and with the frequency band used, from 2.4 GHz to 5 GHz.

Fig. 8 shows the direct output of the method presented in Section III-B1, i.e., h_0 as function of the link distance d. The antenna height design method (blue crosses) is compared against the worst-case height (red circles) as defined before. These plots are very revealing, showing three clear zones in the link distance for each scenario:

- **Far region**, on the right in each plot, corresponding to the two-ray model tail, without nulls and a steady behavior. For such distances, the specific height of the onshore antenna makes little difference and the attenuation increases logarithmically with the link distance. In this region the best height is the top of the range, confirming why this approach is commonly used in practice.
- **Transition region**, in the center in each plot, where the difference between the worst-case and best-case is maximal and a fixed antenna height creates strong variations in attenuation within small changes of the link distance. It corresponds to the area around the last null or few nulls in the two-ray model. This is where our method is more useful allowing a good control of the average attenuation.
- **Near region**, in the left of each plot, where the best and worst average attenuation are rather close together. This is the region in the two-ray model where many nulls appear in close sequence, with high instability of the link. In this case, the onshore antenna heights that produce the best and worst-case attenuation vary almost erratically, but have little impact on the attenuation. Our method is not effective in this region.

Here, we are not providing a numeric way of separating the three regions. However, for each concrete situation, i.e., specific antenna height of the surface node, frequency band used and depth of the tidal cycle, we can run the optimization method and draw the corresponding plots of attenuation and onshore antenna height. Then, the region in which our proposed method is suited for can be easily visually identified.

V. Related Work & Contribution

The recent advances in the Internet of Things (IoT) and next-generation wireless networks are transforming the marine industry and related research activities [1], [21]–[23]. Moored, fixed, drifting, and vehicular aquatic nodes are now part of a rich ecosystem of potentially interconnected aquatic embedded systems with autonomous and/or superior sensing, control and communication capabilities [1], [24]. Wireless technologies play a crucial role in this concept, further enabling novel applications and promising possibilities in different maritime domains (e.g. aquaculture, environmental monitoring, marine transportation, search and rescue). This importance is even higher for industrial, mission-critical or even safety-critical applications, for which more reliable wireless communication performance is required.

At near-shore, the case of onshore stations communicating with floating or semi-floating nodes such as buoys, USVs and AUVs is becoming common, stressing the need for a better understanding of the over-water channel [25], [26]. Yet, more

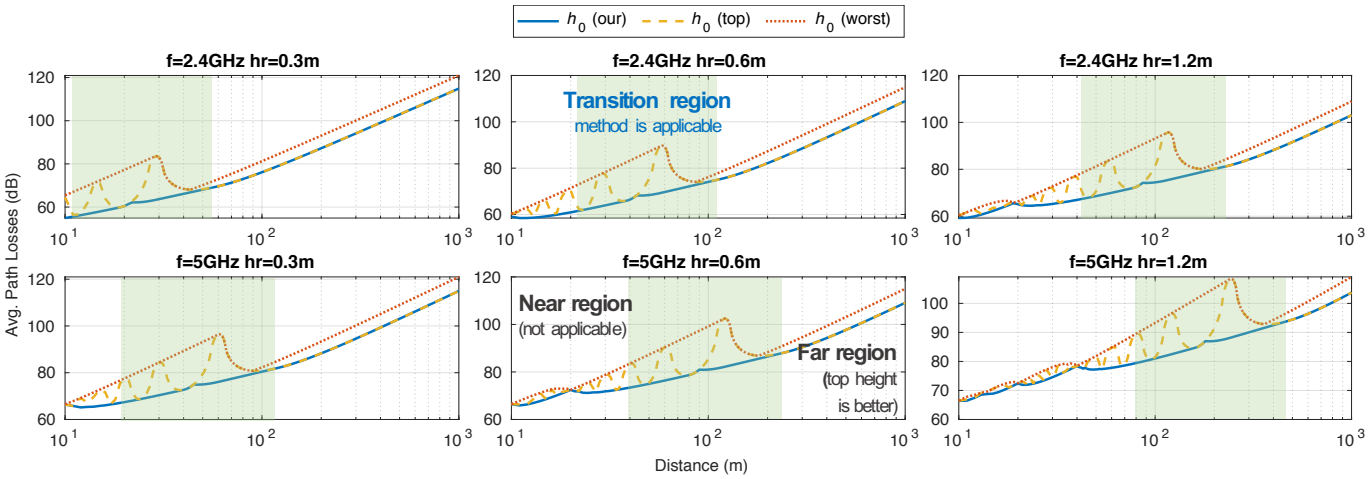

Fig. 7: Link average path loss experienced over a given tidal range as a function of the link distance when using: our antenna-height design method (solid blue), the largest possible antenna height (dashed yellow), or the worst antenna-height (dotted red) for two frequency bands: 2.4 GHz (top row) and 5 GHz (bottom row); and three different heights of surface nodes: 0.3m (left column), 0.6m (middle column) and 1.2m (right column).

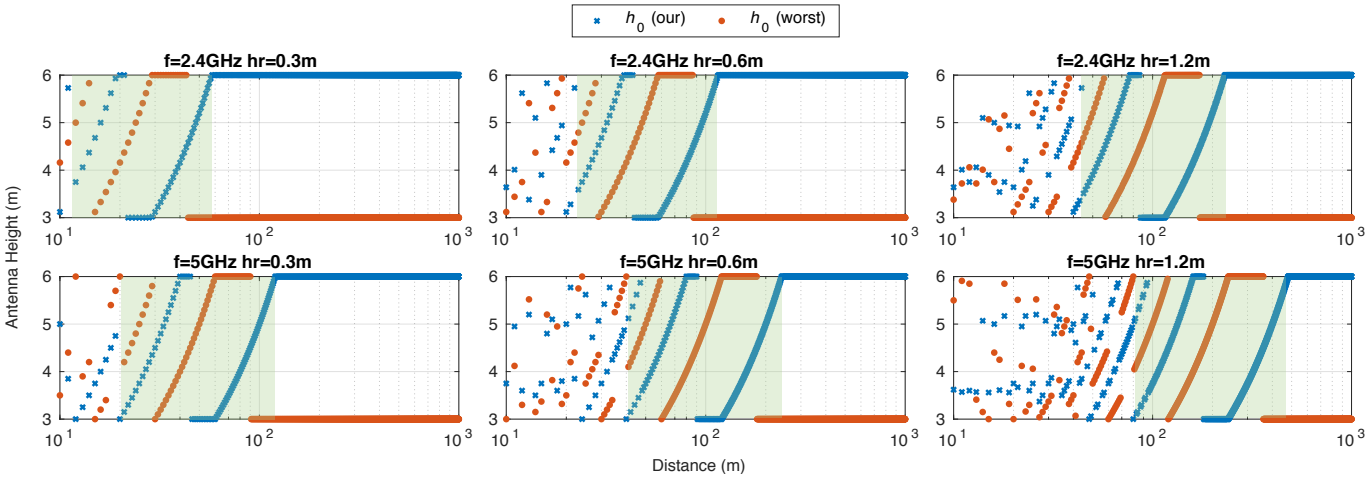

Fig. 8: Onshore antenna height as function of the link distance provided by our antenna-height design method (blue crosses), together with the worst performing antenna height (red circles) within the feasibility range, for two frequency bands: 2.4 GHz (top row) and 5 GHz (bottom row); and three different heights of surface nodes: 0.3m (left column), 0.6m (middle column) and 1.2m (right column).

traditional works in the literature are typically focused on the long-range distances [27]–[29], and rarely consider the case of onshore antennas close to the water surface and at near-shore. Moreover, the impact of tides is often ignored in floating nodes, despite being identified as one of the most detrimental issues in shore-to-shore over-water links [7], [8], [12], [13], [30]. All in all, the gap between the existing literature and the impact of tides on the over-water channel is crystal clear, limited to a few initial works [11], [15], [30]–[32] that try to model and predict the trends on the received signal strength through the two-ray propagation model.

This work contributes to the state-of-the-art in the over-water wireless communication by providing, for the first time, a positioning and antenna height design method to mitigate the impact of tides on the LoS shore-to-surface channel. The experimental results also provide a novel and clear initial validation of the 2-ray model with WiFi technology over water.

VI. Conclusions

This work analyzed the optimal combination of link distance and antenna height for the link design between an onshore station and a surface node over tidal waters. We considered two problems: (A) positioning mobile nodes on the surface, such as AUVs and USVs, to ensure a good quality link at any point of the tide for intense but short duration communication session with a station on shore, and (B) defining the optimal onshore antenna height that minimizes average attenuation over a full tidal cycle when communicating with fixed surface nodes that communicate continuously.

The proposed solutions for both problems are based on the well-known two-ray propagation model. Our experimental results confirmed the validity of this model for shore-to-AUV WiFi links and provided insights for good positioning of the nodes. We also carried out simulations that brought up very relevant details on the onshore antenna height definition to minimize attenuation for continuous communication.

This study and methods target a better design of maritime IoT-driven applications which operate and/or rely on floating or semi-floating nodes on tidal waters, thus requiring the mitigation of path loss degradation due to tidal fading. In the future we plan to refine the models of the components used in the link to further improve the accuracy of the two-ray model and the methods developed on top. We will also carry out the experimental validation of more operational scenarios.

ACKNOWLEDGMENT

This work was partially supported by National Funds through FCT/MCTES (Portuguese Foundation for Science and Technology), within the CISTER Research Unit (UIDP/UIDB/04234/2020) and by FCT through the European Social Fund (ESF) and the Regional Operational Programme (ROP) Norte 2020, under grant 2020.06685.BD, as well as by the European Union's Horizon 2020 *Marine robotics research infrastructure network* project under grant agreement No 731103. This support is gratefully acknowledged.

REFERENCES

[1] A. Zolich, D. Palma, K. Kansanen, K. Fjørtoft, J. Sousa, K. H. Johansson, Y. Jiang, H. Dong, and T. A. Johansen, "Survey on communication and networks for autonomous marine systems," *Journal of Intelligent & Robotic Systems*, vol. 95, no. 3-4, pp. 789–813, 2019.

[2] H. Nam, S. An, C.-H. Kim, S.-H. Park, Y.-W. Kim, and S.-H. Lim, "Remote monitoring system based on ocean sensor networks for offshore aquaculture," in *2014 Oceans-St. John's*, pp. 1–7, IEEE, 2014.

[3] A. Gaugue, M. Menard, E. Migot, P. Bourcier, and C. Gaschet, "Development of an aquatic USV with high communication capability for environmental surveillance," in *OCEANS 2019-Marseille*, pp. 1–8, IEEE, 2019.

[4] K. E. Fjørtoft, F. Bekkadal, and P. Kabacik, "Maritime operations in arctic waters," in *2013 MTS/IEEE OCEANS-Bergen*, pp. 1–8, IEEE, 2013.

[5] J. Wang, H. Zhou, Y. Li, Q. Sun, Y. Wu, S. Jin, T. Q. Quek, and C. Xu, "Wireless channel models for maritime communications," *IEEE Access*, vol. 6, pp. 68070–68088, 2018.

[6] T. Rappaport, *Wireless Communications: Principles and Practice*. USA: Prentice Hall PTR, 2nd ed., 2002.

[7] M. Pereira, "Spread spectrum techniques in wireless communication part 2: Transmission issues in free space," *IEEE Instrumentation & Measurement Magazine*, vol. 13, no. 1, pp. 8–14, 2010.

[8] A. LaGrone, A. Straiton, and H. Smith, "Synthesis of radio signals on overwater paths," *IRE Trans. on Antennas and Propagation*, vol. 3, no. 2, pp. 48–52, 1955.

[9] C.-W. Ang and S. Wen, "Signal strength sensitivity and its effects on routing in maritime wireless networks," in *2008 33rd IEEE Conference on Local Computer Networks (LCN)*, pp. 192–199, IEEE, 2008.

[10] Y. Huo, X. Dong, and S. Beatty, "Cellular communications in ocean waves for maritime internet of things," *IEEE Internet of Things Journal*, vol. 7, no. 10, pp. 9965–9979, 2020.

[11] M. G. Gaitán, L. Pinto, P. M. Santos, and L. Almeida, "On the two-ray model analysis for overwater links with tidal variations," in *2019 11th National Symposium on Informatics (INFORUM)*, 2019.

[12] D. Taplin, "Tidal fading on short oversea paths elliptical, vertical and horizontal polarisation compared," *NASA STI/Recon Technical Report N*, vol. 76, p. 15328, 1975.

[13] A. Macmillan, M. K. Marina, and J. T. Triana, "Slow frequency hopping for mitigating tidal fading on rural long distance over-water wireless links," in *2010 IEEE Conference on Computer Communications (INFOCOM) Workshops*, pp. 1–5, IEEE, 2010.

[14] N. Fuke, K. Sugiyama, and H. Shinonaga, "Long-range oversea wireless network using 2.4 GHz wireless LAN installation and performance," in *Proc. of the 12th Int'l Conf. on Computer Communications and Networks*, pp. 351–356, IEEE, 2003.

[15] M. G. Gaitán, P. M. Santos, L. Pinto, and L. Almeida, "Optimal antenna-height design for improved capacity on over-water radio links affected by tides," in *Global OCEANS 2020: Singapore–US Gulf Coast*, IEEE, 2020.

[16] S. Basagni, L. Bölöni, P. Gjanci, C. Petrioli, C. A. Phillips, and D. Turgut, "Maximizing the value of sensed information in underwater wireless sensor networks via an autonomous underwater vehicle," in *IEEE INFOCOM 2014-IEEE Conference on Computer Communications*, pp. 988–996, IEEE, 2014.

[17] T. Zugno, F. Campagnaro, and M. Zorzi, "Controlling in real-time an ASV-carried ROV for quay wall and ship hull inspection through wireless links in harbor environments," in *Global Oceans 2020: Singapore–US Gulf Coast*, pp. 1–9, IEEE, 2020.

[18] Z. Yang, M. Li, and Y. Liu, "Sea depth measurement with restricted floating sensors," in *28th IEEE International Real-Time Systems Symposium (RTSS 2007)*, pp. 469–478, IEEE, 2007.

[19] I. Bennis, A. Gaugue, and M. Menard, "Short-range and long-range cooperative communication for littoral environment monitoring," in *2019 15th International Wireless Communications & Mobile Computing Conference (IWCMC)*, pp. 1958–1963, IEEE, 2019.

[20] OceanScan-MST, "Light autonomous underwater vehicle." https://www.oceanscan-mst.com/light-autonomous-underwater-vehicle/, 2021.

[21] G. Xu, Y. Shi, X. Sun, and W. Shen, "Internet of things in marine environment monitoring: A review," *Sensors*, vol. 19, no. 7, p. 1711, 2019.

[22] S. Guan, J. Wang, C. Jiang, R. Duan, Y. Ren, and T. Q. Quek, "MagicNet: The maritime giant cellular network," *IEEE Communications Magazine*, vol. 59, no. 3, pp. 117–123, 2021.

[23] J. Waterston, J. Rhea, S. Peterson, L. Bolick, J. Ayers, and J. Ellen, "Ocean of things : Affordable maritime sensors with scalable analysis," in *OCEANS 2019 - Marseille*, pp. 1–6, 2019.

[24] J. Baghdady, M. Incze, P. Dias, K. Lima, A. Z. Trimble, N. Hafner, R. Andrade, M. Costa, M. Ribeiro, J. Sousa, *et al.*, "Enabling interoperability among disparate unmanned vehicles via coordinated command, control, and communications strategies," in *Global Oceans 2020: Singapore–US Gulf Coast*, pp. 1–5, IEEE, 2020.

[25] B. Yamamoto, A. Wong, P. J. Agcanas, K. Jones, D. Gaspar, R. Andrade, and A. Z. Trimble, "Received signal strength indication (RSSI) of 2.4 GHz and 5 GHz wireless local area network systems projected over land and sea for near-shore maritime robot operations," *Journal of Marine Science and Engineering*, vol. 7, no. 9, p. 290, 2019.

[26] Y. Wang, X. Zheng, L. Liu, and H. Ma, "PolarTracker: Attitude-aware channel access for floating low power wide area networks," in *IEEE INFOCOM 2021-IEEE Conference on Computer Communications*, pp. 1–10, IEEE, 2021.

[27] T. Røste, K. Yang, and F. Bekkadal, "Coastal coverage for maritime broadband communications," in *2013 MTS/IEEE OCEANS-Bergen*, pp. 1–8, IEEE, 2013.

[28] R. Raulefs, M. Wirsing, and W. Wang, "Increasing long range coverage by multiple antennas for maritime broadband communications," in *OCEANS 2018 MTS/IEEE Charleston*, pp. 1–6, IEEE, 2018.

[29] F. B. Teixeira, R. Campos, and M. Ricardo, "Height optimization in aerial networks for enhanced broadband communications at sea," *IEEE Access*, vol. 8, pp. 28311–28323, 2020.

[30] J. Cecílio, P. M. Ferreira, and A. Casimiro, "Evaluation of LoRa technology in flooding prevention scenarios," *Sensors*, vol. 20, no. 14, p. 4034, 2020.

[31] M. G. Gaitán, P. M. Santos, L. Pinto, and L. Almeida, "Experimental evaluation of the two-ray model for near-shore WiFi-based network systems design," in *91st Vehicular Technology Conference (VTC)*, IEEE, 2020.

[32] H. Taka and M. Wada, "Tidal level estimation using a 5GHz band wireless access system," in *2015 International Symposium on Antennas and Propagation (ISAP)*, pp. 1–4, IEEE, 2015.